Proceedings of ALGORITMY 2012
pp. 438–447

STABILIZED SEMI-IMPLICIT FINITE VOLUME SCHEME FOR PARABOLIC TENSOR DIFFUSION EQUATIONS

ANGELA HANDLOVIČOVÁ, PAVOL KÚTIK, KAROL MIKULA *

Abstract. We introduce a new stabilized finite volume method for solving tensor diffusion equations. The new scheme is based on the classical diamond-cell finite volume method and on the idea of inflow-implicit/outflow-explicit (or forward-backward diffusion) splitting accompanied by a suitable stabilization. Comparisons with known exact solution and numerical experiments investigating stability of the proposed method in case of highly anisotropic diffusion tensor are discussed.

Key words. tensor diffusion, finite volume method, diamond-cell scheme, stabilization, inflow-implicit/outflow-explicit scheme

AMS subject classifications. 35K20, 65M08, 65M12

1. Introduction. The goal of this article is to present new numerical method for solving tensor diffusion equation of the form

$$\frac{\partial u}{\partial t} = \nabla \cdot (\mathbf{D}\nabla u), \tag{1.1}$$

where $u : \mathbb{R}^2 \times [0, T] \to \mathbb{R}$ is an unknown function and $\mathbf{D}$ is a positive–definite diffusion matrix. The equation (1.1) is accompanied by initial and boundary conditions, either of Dirichlet or Neumann type. For the sake of simplicity we restrict our presentation only to a constant coefficient two-dimensional case, i.e.

$$\mathbf{D} = \begin{pmatrix} d_{11} & d_{12} \\ d_{21} & d_{22} \end{pmatrix}, \tag{1.2}$$

but the method can be applied to a more general cases where matrix $\mathbf{D}$ may depend on spatial position $\mathbf{x} = (x, y)$ and/or on the solution u. The tensor diffusion equations arise in many applications like the heat transfer in anisotropic media, porous media flow in anisotropic layers, coherence enhancing image filtering or in stochastic volatility based derivative pricing in financial mathematics.

The numerical scheme presented in this article is based on the so-called diamond-cell finite volume scheme, see e.g. [2, 4]. The diamond-cell scheme for solving tensor diffusion elliptic problems was studied in [2] and convergence and error estimates for nonlinear parabolic tensor diffusion equations were given in [4, 5]. In our new approach, the classical diamond-cell scheme is rewritten into a form where we can identify forward and backward diffusion coefficients governing diffusion fluxes between finite volume p and its neighbours q. Using the idea of Mikula and Ohlberger [7] we split the scheme into a forward diffusion part which is treated implicitly and to a backward diffusion part which is treated explicitly. By the analogy to finite volume

*Department of Mathematics and Descriptive Geometry, Slovak University of Technology, Bratislava, Slovak Republic, (angela@math.sk, pavol.kutik@gmail.com, mikula@math.sk).

This work was supported by grants VEGA 1/1137/12 and APVV-0184-10.

schemes for advection equations [8, 9] we shall call this forward-backward/implicit-explicit diffusion splitting as the inflow-implicit/outflow-explicit (IIOE) scheme. Interestingly, such splitting has the same order of accuracy as the original diamond-cell scheme, which will be shown computationally on a representative example of exact solution to the problem. The inflow-implicit/outflow-explicit (or forward-backward diffusion) splitting brings always diagonally dominant M-matrix of the arising linear system which yields good solvability and stability properties of the implicit part of the scheme. On the other hand, the implicit part does not always "dominate" the explicit part of the scheme and some spurious oscillations related to backward diffusion (outflow) coefficients may appear. In order to build L_∞-stable scheme fulfilling discrete minimum-maximum principle we use stabilization presented in [10] where high-resolution schemes were built for solving advection equations. The stabilization is based on the so-called flux-corrected transport methodology [1, 11] which is in our case applied only to the explicit part of the scheme (see also [6]) and only in finite-volumes where the local discrete minimum-maximum principle is violated after application of the basic IIOE scheme (see also [10]). Since such stabilization is performed in a two step procedure we call it S^2IIOE scheme. Our numerical experiments show that S^2IIOE scheme seems to be suitable for solving anisotropic diffusion problems since it supresses the spurious oscillations and do not touch significantly the non-oscilatory part of solution of the original IIOE scheme.

The paper is organized as follows. In section 2 we repeat the formulation of the standard diamond-cell finite volume scheme on a simple squared grid in two dimensions. Then we present its IIOE splitting and our stabilization method. In Section 3 we discuss experimental order of convergence of the presented numerical schemes and present examples where the effect of stabilization is studied in order to fulfill discrete minimum-maximum principle. Finally some concluding remarks are made.

2. Numerical schemes. We consider equation (1.1) in a bounded rectangular domain $\Omega \subset \mathbb{R}^2$ and time interval $I = [0, T]$. We consider an admissible mesh $\mathcal{T}_h$, in the sense of [3], consisting for simplicity only of squared finite volumes. Let p be a finite volume and σ_{pq} be an edge between p and q, $q \in N(p)$, where $N(p)$ is set of all neighbouring cells, i.e. finite volumes which have a common one-dimensional face with p. The set $N'(p)$ denotes all finite volumes which have either a common edge or a common vertex with the cell p. Obviously $N(p) \subset N'(p)$ and in two dimensions $\mathrm{card}(N(p)) = 4$ whereas $\mathrm{card}(N'(p)) = 8$. In particular, the set $N'(p) = \{e, ne, n, nw, w, sw, s, se\}$ denotes east, north-east, north, north-west, west, south-west, south and south-east neighbouring cell of the finite volume p. Since all finite volumes are equal squares, length of any edge σ_{pq} is denoted by h. Let the center of each cell (finite volume) p be denoted by $\mathbf{x}_p$ and the intersection point of σ_{pq} and line connecting $\mathbf{x}_p$ and $\mathbf{x}_q$, $q \in N(p)$ be denoted by $\mathbf{x}_{pq}$. Such definition complies with the definition of an admissible mesh where each line joining $\mathbf{x}_p$ and $\mathbf{x}_q$, $q \in N(p)$, must be orthogonal to σ_{pq}. We denote this orthonormal direction, i.e. the unit outer normal vector to σ_{pq} with respect to p, by $\mathbf{n}_{pq}$. Clearly, the distance between two neighbouring cell centers is $|\mathbf{x}_p - \mathbf{x}_q| = h$. Furthermore the measure of every finite volume equals to h^2. We use uniform discrete time step τ in order to discretize the time interval $[0, T]$. The numerical solution inside a finite volume p at time step n is denoted by u_p^n.

2.1. Diamond-cell finite volume scheme. In order to motivate our new scheme let us first recall the well-known diamond-cell method used for solving tensor diffusion equations. Integrating (1.1) over the finite volume p and applying Green's theorem to the right-hand side yields

$$\int_p \frac{\partial u}{\partial t}\,\mathrm{d}x = \sum_{q\in N(p)} \int_{\sigma_{pq}} \begin{pmatrix} d_{11}\frac{\partial u}{\partial x} + d_{12}\frac{\partial u}{\partial y} \\ d_{21}\frac{\partial u}{\partial x} + d_{22}\frac{\partial u}{\partial y} \end{pmatrix} \cdot \mathbf{n}_{pq}\,\mathrm{d}s. \tag{2.1}$$

As the mesh consists of squares with edges parallel to the coordinate system we can easily rewrite (2.1) into the following form

$$\begin{aligned}\int_p \frac{\partial u}{\partial t}\,\mathrm{d}x = &\int_{\sigma_{pe}} \left(d_{11}\frac{\partial u}{\partial x} + d_{12}\frac{\partial u}{\partial y}\right)\mathrm{d}\gamma + \int_{\sigma_{pn}} \left(d_{21}\frac{\partial u}{\partial x} + d_{22}\frac{\partial u}{\partial y}\right)\mathrm{d}\gamma - \\ &\int_{\sigma_{pw}} \left(d_{11}\frac{\partial u}{\partial x} + d_{12}\frac{\partial u}{\partial y}\right)\mathrm{d}\gamma - \int_{\sigma_{ps}} \left(d_{21}\frac{\partial u}{\partial x} + d_{22}\frac{\partial u}{\partial y}\right)\mathrm{d}\gamma\end{aligned} \tag{2.2}$$

where $\sigma_{pe}, \sigma_{pn}, \sigma_{pw}, \sigma_{ps}$ denote the east, north, west and south edge of an arbitrary interior finite volume p.

In the discretized version we replace the time derivative in (2.2) by the backward difference in a representative point $\mathbf{x}_p$ and use a central-difference-like approximations for the space derivatives, e.g. for the edge σ_{pe} it looks

$$\frac{\partial u}{\partial x}(\mathbf{x}_{pe}) \approx \frac{u_e - u_p}{h},\ \frac{\partial u}{\partial y}(\mathbf{x}_{pe}) \approx \frac{1}{2}\left(\frac{u_n - u_s}{2h} + \frac{u_{ne} - u_{se}}{2h}\right). \tag{2.3}$$

Let us note that these approximations can be generalized to non-rectangular meshes in two or three dimensions by using gradient approximation on a diamond-like shape around the edge σ_{pe} from which the method took its name. Following such approximations we get

$$\begin{aligned}\frac{u_p^n - u_p^{n-1}}{\tau}h^2 = {} & d_{11}\,(u_e^n - u_p^n) + \frac{d_{12}}{4}(u_{ne}^n - u_{se}^n + u_n^n - u_s^n) + \\ & \frac{d_{21}}{4}(u_{ne}^n - u_{nw}^n + u_e^n - u_w^n) + d_{22}(u_n^n - u_p^n) + \\ & d_{11}\,(u_w^n - u_p^n) + \frac{d_{12}}{4}(u_{sw}^n - u_{nw}^n + u_s^n - u_n^n) + \\ & \frac{d_{21}}{4}(u_{sw}^n - u_{se}^n + u_w^n - u_e^n) + d_{22}(u_s^n - u_p^n).\end{aligned}$$

which can be further simplified to obtain the standard diamond-cell scheme

$$\begin{aligned}&\frac{h^2}{\tau}u_p^n + d_{11}(u_p^n - u_e^n) + \frac{d_{12}}{4}(u_{se}^n - u_{ne}^n) + \frac{d_{21}}{4}(u_{nw}^n - u_{ne}^n) + d_{22}(u_p^n - u_n^n) + \\ &d_{11}(u_p^n - u_w^n) + \frac{d_{12}}{4}(u_{nw}^n - u_{sw}^n) + \frac{d_{21}}{4}(u_{se}^n - u_{sw}^n) + d_{22}(u_p^n - u_s^n) = \frac{h^2}{\tau}u_p^{n-1}\end{aligned} \tag{2.4}$$

2.2. Inflow-implicit/outflow-explicit (IIOE) scheme. Let us add and subtract the term u_p^n to each expression in parentheses on the left-hand side and collect all coefficients which multiply the same expression $(u_p^n - u_q^n)$, where $q \in N'(p)$. Then the diamond-cell scheme (2.4) can be written as follows

$$u_p^n + \frac{\tau}{h^2}\sum_{q\in N'(p)} a_{pq}(u_p^n - u_q^n) = u_p^{n-1}, \tag{2.5}$$

where

$$a_{pe} = a_{pw} = d_{11},\ a_{pn} = a_{ps} = d_{22}, \tag{2.6}$$

$$a_{pnw} = a_{pse} = -\frac{d_{12}+d_{21}}{4},\ a_{pne} = a_{psw} = \frac{d_{12}+d_{21}}{4}. \tag{2.7}$$

Assuming non-diagonal anisotropic positive definite diffusion matrix, we know that d_{11} and d_{22} are always positive but we also see that the pairs of coefficients in (2.7) have opposite signs but the same magnitude. These facts may violate the M-matrix property and diagonal-dominance of the system matrix and cause that its inverse is not positive matrix (i.e. matrix with only non-negative entries) with raw-sum equals to 1. Non-positiveness of the inverse matrix may cause or magnify spurious oscillations and thus violate the minimum-maximum principle in numerical solution which is always fulfilled in the case of continuous solution. We are able to treat these undesired situations by applying the so-called inflow-implicit/outflow-explicit splitting of the original diamond-cell scheme. To that goal, the basic scheme (2.5) is adjusted so that all diffusion fluxes with positive coefficients $a_{pq} \geq 0$ are treated implicitly and all diffusion fluxes with negative coefficients $a_{pq} < 0$ are taken explicitly. In such a way we obtain the basic IIOE scheme for tensor diffusion

$$u_p^n + \frac{\tau}{h^2} \sum_{q \in N'(p)} a_{pq}^{in}(u_p^n - u_q^n) = u_p^{n-1} - \frac{\tau}{h^2} \sum_{q \in N'(p)} a_{pq}^{out}(u_p^{n-1} - u_q^{n-1}), \tag{2.8}$$

where

$$a_{pe}^{in} = a_{pw}^{in} = d_{11},\ a_{pn}^{in} = a_{ps}^{in} = d_{22}$$
$$a_{pnw}^{in} = a_{pse}^{in} = \max\left(-\frac{d_{12}+d_{21}}{4}, 0\right),\ a_{pne}^{in} = a_{psw}^{in} = \max\left(\frac{d_{12}+d_{21}}{4}, 0\right)$$

and

$$a_{pe}^{out} = a_{pw}^{out} = 0,\ a_{pn}^{out} = a_{ps}^{out} = 0$$
$$a_{pnw}^{out} = a_{pse}^{out} = \min\left(-\frac{d_{12}+d_{21}}{4}, 0\right),\ a_{pne}^{out} = a_{psw}^{out} = \min\left(\frac{d_{12}+d_{21}}{4}, 0\right).$$

In this way we obtain a system matrix which is diagonally dominant M-matrix for which the system is always solvable and which inverse is always positive. The only part of this scheme which may cause a failure of the discrete minimum-maximum principle is the outflow-explicit (backward diffusion) right hand side since it may happen that in some situations the inflow-implicit (forward diffusion) part does not have an enough strength to keep numerical solution in the initially given range of solution values.

2.3. Stabilized IIOE scheme for tensor diffusion. The stabilization of the IIOE scheme (2.8) is based on strategy presented in [10]. It consists in assigning weights to the outflow (backward diffusion) coefficients in order to keep the righ-hand side in a desired range and correspondingly adjusting the inflow (forward diffusion) coefficients. We can write the stabilized scheme in the following general form

$$u_p^n + \frac{\tau}{h^2} \sum_{q \in N'(p)} A_{pq}^{in}(u_p^n - u_q^n) = u_p^{n-1} - \frac{\tau}{h^2} \sum_{q \in N'(p)} \theta_{pq}^{out}\, a_{pq}^{out}(u_p^{n-1} - u_q^{n-1}) \tag{2.9}$$

with outflow weighting factors $\theta_{pq}^{out} \in [0,1]$ and corrected inflows A_{pq}^{in} given by the strategy explained below.

It is clear that if the following two conditions

$$u_p^{n-1} - \frac{\tau}{h^2} \sum_{q \in N'(p)} \theta_{pq}^{out}\, a_{pq}^{out} (u_p^{n-1} - u_q^{n-1}) \le u_p^{max,n-1}, \tag{2.10}$$

$$u_p^{n-1} - \frac{\tau}{h^2} \sum_{q \in N'(p)} \theta_{pq}^{out}\, a_{pq}^{out} (u_p^{n-1} - u_q^{n-1}) \ge u_p^{min,n-1}, \tag{2.11}$$

with $u_p^{max,n-1} = \max\{u_p^{n-1}, \{u_q^{n-1}, q \in N'(p)\}\}$, $u_p^{min,n-1} = \min\{u_p^{n-1}, \{u_q^{n-1}, q \in N'(p)\}\}$, are fulfilled in every finite volume p then the numerical solution fulfills the discrete minimum-maximum principle. In order to have conditions (2.10) and (2.11) satisfied it is sufficient that the following two inequalities

$$\frac{u_p^{n-1}}{n^{out}} - \frac{\tau}{h^2} \theta_{pq}^{out}\, a_{pq}^{out} (u_p^{n-1} - u_q^{n-1}) \le \frac{u_p^{max,n-1}}{n^{out}}, \tag{2.12}$$

$$\frac{u_p^{n-1}}{n^{out}} - \frac{\tau}{h^2} \theta_{pq}^{out}\, a_{pq}^{out} (u_p^{n-1} - u_q^{n-1}) \ge \frac{u_p^{min,n-1}}{n^{out}} \tag{2.13}$$

hold for every $q \in N'(p)$ where $a_{pq}^{out}(u_p^{n-1} - u_q^{n-1}) \neq 0$. The symbol n_p^{out} denotes the number of nonzero outflows from the finite volume p to all its neighbours, i.e.

$$n_p^{out} = \sum_{q \in N'(p)} \mathrm{abs}\,(\mathrm{sign}(a_{pq}^{out}\,(u_p^{n-1} - u_q^{n-1}))). \tag{2.14}$$

Clearly, if we sum (2.12), respectively (2.13), over all $q \in N'(p)$, we obtain (2.10), respectively (2.11). It remains to define the coefficients θ_{pq}^{out} which would satisfy (2.12)-(2.13) and it can be done as follows

$$\theta_{pq}^{out} = \min\left(1, \frac{h^2(u_p^{max,n-1} - u_p^{n-1})}{\tau n_p^{out} a_{pq}^{out}(u_q^{n-1} - u_p^{n-1})}\right), \quad \text{if} \quad a_{pq}^{out}(u_q^{n-1} - u_p^{n-1}) > 0, \tag{2.15}$$

$$\theta_{pq}^{out} = \min\left(1, \frac{h^2(u_p^{min,n-1} - u_p^{n-1})}{\tau n_p^{out} a_{pq}^{out}(u_q^{n-1} - u_p^{n-1})}\right), \quad \text{if} \quad a_{pq}^{out}(u_q^{n-1} - u_p^{n-1}) < 0, \tag{2.16}$$

$$\theta_{pq}^{out} = 1, \qquad \text{if} \quad a_{pq}^{out}(u_q^{n-1} - u_p^{n-1}) = 0. \tag{2.17}$$

By using these definitions we have reduced the otflow coefficients in the scheme (2.9) by the factor $(1 - \theta_{pq}^{out}) a_{pq}^{out}$ which must be added to the inflows of the neighbours. To that goal we define

$$A_{qp}^{in} = a_{qp}^{in} - (1 - \theta_{pq}^{out}) a_{pq}^{out} \tag{2.18}$$

what determines the new inflow coefficients in the scheme (2.9).

Our final numerical scheme is a two-step combination of (2.8) and (2.9). It relies on the fact that in rather general cases the IIOE scheme (2.8) does not need any stabilization in order to fulfill the discrete minimum-maximum principle. Hence, in the first step we solve (2.8). In the second step we recalculate the coefficients θ_{pq}^{out} and A_{qp}^{in} according to (2.15) - (2.18), but only in finite volumes p where the local minimum-maximum principle was violated, and resolve the problem using the scheme (2.9). We call this algorithm S^2IIOE and summarize it as follows:

TABLE 3.1
Errors in $L_2(I,\Omega)$ norm and EOCs for the schemes for the exact solution (3.1)

.

n_x, n_y	DIAMOND-CELL	EOC	IIOE	EOC	S^{2}IIOE	EOC
20	$1.76\ \ 10^{-2}$	-	$1.05\ \ 10^{-2}$	-	$1.04\ \ 10^{-2}$	-
40	$8.09\ \ 10^{-3}$	1.12	$5.63\ \ 10^{-3}$	0.90	$5.56\ \ 10^{-3}$	0.90
80	$2.85\ \ 10^{-3}$	1.50	$2.25\ \ 10^{-3}$	1.32	$2.27\ \ 10^{-3}$	1.29
160	$8.21\ \ 10^{-4}$	1.79	$6.78\ \ 10^{-4}$	1.74	$7.14\ \ 10^{-4}$	1.67
320	$1.88\ \ 10^{-4}$	2.13	$1.57\ \ 10^{-4}$	2.11	$1.92\ \ 10^{-4}$	1.89

S^{2}IIOE scheme for tensor diffusion:

1. solve (2.9) with $\theta_{pq}^{out} = 1, A_{pq}^{in} = a_{pq}^{in}$
2. if $u_p^n > u_p^{max,n-1}$ or $u_p^n < u_p^{min,n-1}$, redefine θ_{pq}^{out} and A_{qp}^{in} according to (2.15) – (2.18) and solve (2.9).

3. Numerical experiments. In this section we first compare the experimental order of convergence (EOC) of the above described methods using the exact solution to the equation (1.1) with inhomogeneous Dirichlet boundary conditions. In the second subsection we discuss stability features of the schemes on the example when an initial impulse diffuses given zero Neumann boundary conditions. We discretize the computational domain $[-x_L, x_R] \times [-y_L, y_R]$ into $n_x \times\ n_y$ finite volumes and the time interval $[0, T]$ into n_{ts} time steps such that $h = (x_R - x_L)/n_x = (y_R - y_L)/n_y$, $\tau = T/n_{ts}$. The solution of the arising linear systems is computed by the standard SOR algorithm. The diffusion tensor for both experiments is given by the matrix

$$\mathbf{D} = \begin{pmatrix} 2 & 1.99 \\ 1.99 & 2 \end{pmatrix}.$$

with eigenvectors $(\frac{\sqrt{2}}{2}, \frac{\sqrt{2}}{2})^T$ and $(-\frac{\sqrt{2}}{2}, \frac{\sqrt{2}}{2})^T$ and eigenvalues 3.99 and 0.01 thus the diffusion is much stronger in the diagonal direction $y = x$.

3.1. Comparison with exact solution. Numerical experiments in this part are done using the exact solution to the problem (1.1) which has, for a symmetric positive-definite matrix $\mathbf{D}$, the form

$$u(\mathbf{x}, t) = \frac{1}{4\pi t\sqrt{|\mathbf{D}|}} \exp \frac{\mathbf{x}^T \mathbf{D}^{-1} \mathbf{x}}{4t} \tag{3.1}$$

where $|\mathbf{D}|$ denotes determinant and $\mathbf{D}^{-1}$ inverse of the matrix $\mathbf{D}$. The Dirichlet boundary conditions are determined according to (3.1). The computational domain is $\Omega = [-1, 1] \times [-1, 1]$, $T = 0.1$ and as the initial condition we take $u(\mathbf{x}, 1)$ from (3.1). The time and space discretization is such that the coupling $\tau = h^2$ and $n_x = n_y$ hold.

In Table 3.1 one can see that for such smooth solution (but strongly anisotropic diffusion tensor) all the schemes tend to be second order accurate when refining the grid. Interestingly, the inflow-implicit/outflow-explicit splitting does not bring any additional error but slightly improved the absolute errors in $L_2(I, \Omega)$ norm in this example. Since the stabilization is really performed in a subset of all finite volumes we can observe slower convergence to EOC=2 in case of S^{2}IIOE scheme which is in accordance with our expectations and observable property of high-resolution schemes.

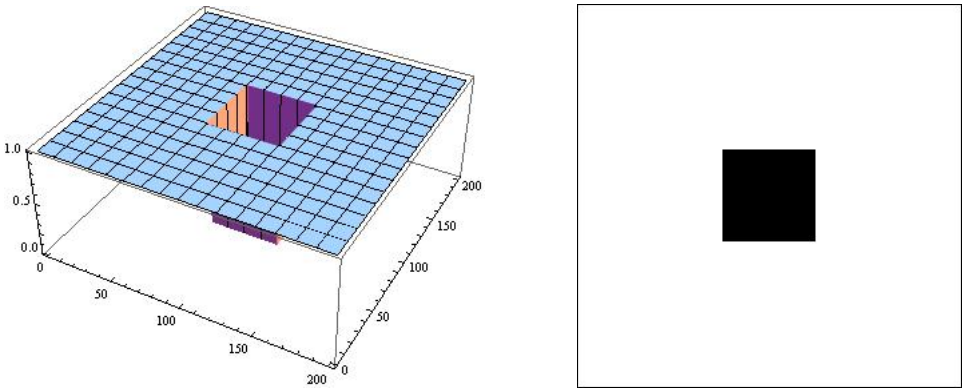

FIG. 3.1. *The piecewise constant initial condition - 3D graph (left) and corresponding 2D image (right).*

3.2. Experiment related to discrete minimum-maximum principle. In this experiment we use the same computational domain and coupling between space and time step as above but the initial condition is a piecewise constant function with the value $u(\mathbf{x}, 0) = 0$ in the region $[-0.25, 0.25] \times [-0.25, 0.25]$ and with $u(\mathbf{x}, 0) = 1$ outside it. The initial condition is plotted in Figure 3.1 as 3D graph (left) and as 2D image (right). We compare the standard diamod-cell and S^2IIOE schemes on the evolution of this piecewise constant initial profile, the results are presented in Figures 3.2-3.6 for computational grid with $n_x = n_y = 200$. The diamond-cell scheme produces some oscillations (the numerical solution becomes slightly greater than 1, see also Figure 3.5) and we highlight such regions using transformation $\bar{u}(\mathbf{x}, t) = u(\mathbf{x}, t) - 1$. After this transformation the oscillatory regions are visible as the black color stripes in 2D image plots of $\bar{u}(\mathbf{x}, t)$. While the overall maximum in all time steps for the diamod-cell scheme was 1.016993, for the S^2IIOE it was 1.0. As one can see from the numerical results, the S^2IIOE scheme removes the oscillations and keep the shape of non-oscillatory part of the solution in right way. It also fulfills strictly the global discrete minimum-maximum principle. In Figure 3.5 we compare visually one cross-section documenting such oscillatory behaviour of the standard diamond-cell scheme and non-oscillatory behaviour of the S^2IIOE scheme. In Figure 3.6 we show the strongly anisotropic profile with shock-like lines formed after 50 time steps of the tensor diffusion computed by S^2IIOE scheme.

Another interesting question is the mass conservation for the stabilized version of the schemes which are conservative (both diamond-cell and IIOE fulfill such property). For the S^2IIOE scheme we got the mass errors 0.00153, 0.000458, 0.000154 and 0.0000565 when refining the grids by using $n_x = n_y = 100, 200, 400, 800$. It shows the convergence in mass conservation of order 1, tending to 1 from above in this example. We note that in more complicated piecewise constant initial profile experiments with zero Neumann boundary conditions we observed convergence order in mass error tending to 1 from below, so the stabilized version seems to fulfill the mass conservation property with order 1 in general.

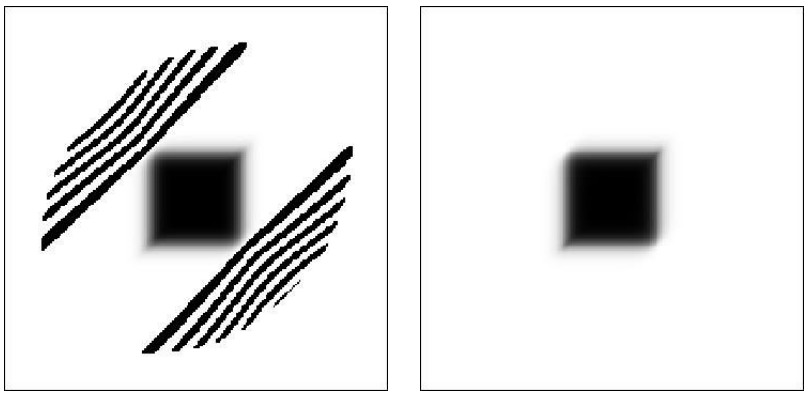

FIG. 3.2. *2D images of tensor diffusion result computed by the standard diamond-cell scheme (left) and* S^2IIOE *scheme (right) at the 4th time step.*

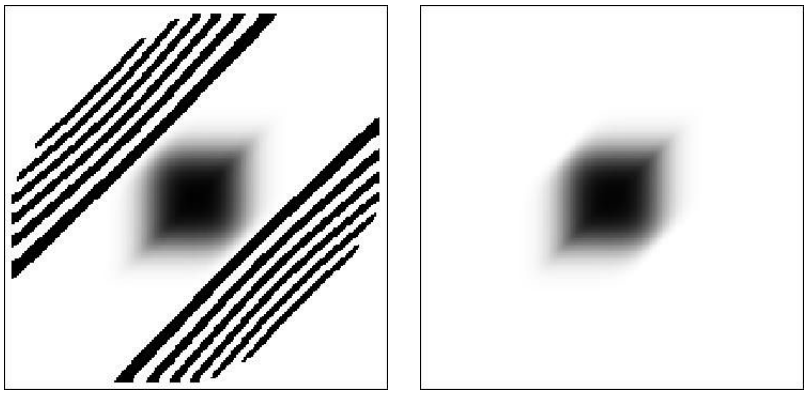

FIG. 3.3. *2D images of tensor diffusion result computed by the standard diamond-cell scheme (left) and* S^2IIOE *scheme (right) at the 20th time step.*

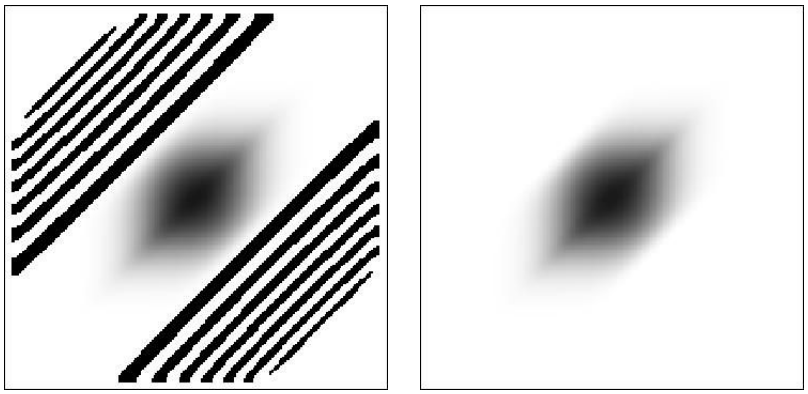

FIG. 3.4. *2D images of tensor diffusion result computed by the standard diamond-cell scheme (left) and* S^2IIOE *scheme (right) at the 50th time step.*

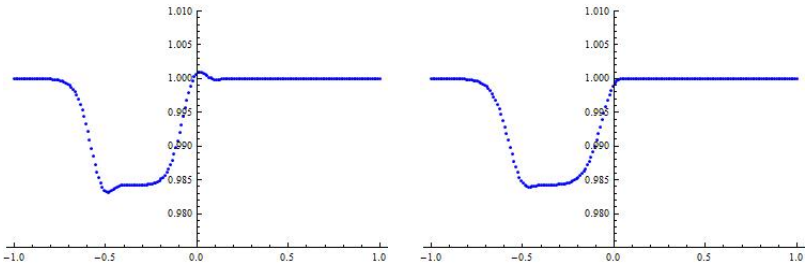

FIG. 3.5. *Cross-section of the numerical solution profile at* $x = -0.55$ *in the 50th time step - result of the standard diamond-cell scheme (left) and result of the* S^2IIOE *scheme (right).*

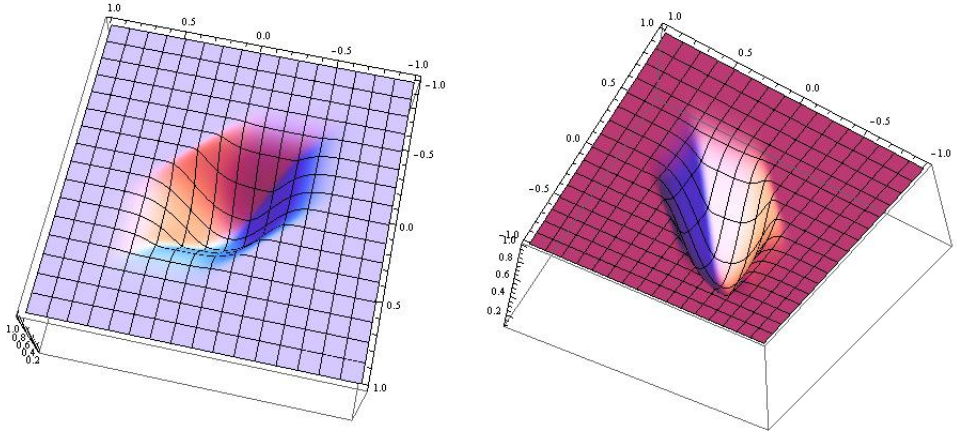

FIG. 3.6. *The solution of tensor diffusion computed by* S^2IIOE *scheme in the 50th time step, the top view (left) and bottom view (right).*

4. Conclusions. In this article we introduced a new stabilized semi-implicit finite volume scheme for solving tensor diffusion equations. It is based on inflow-implicit/outflow-explicit (IIOE) splitting of the standard diamond-cell method and stabilization by a two-step procedure by decreasing outflow coefficients in finite volumes where the application of the basic IIOE scheme violates the local discrete minimum-maximum principle and increasing inflow coefficients of their neighbours. Since such stabilization decreases the range of the right hand side of the system and increases the diffusive properties of the system matrix, we do not expect that any further local oscillations appear after the second step. Although this statement is not studied theoretically yet, it coincides with our observations performing numerical experiments. We studied the experimental convergence order of the new scheme and showed that it is same as for the non-stabilized method in case of the smooth exact solution. We have also shown non-oscillatory behaviour of the new scheme in case of piecewise constant initial profile and strongly anisotropic diffusion tensor. A further study of the proposed numerical scheme will be an objective of our research in the near future.

REFERENCES

[1] J.P.Boris, D.L.Book, Flux-corrected transport: I. SHASTA, a fluid transport algorithm that works, J. Comput. Phys., 11 (1973), pp. 38-69

[2] Y.Coudiere, J. P.Vila, P.Villedieu, Convergence rate of a finite volume scheme for a two-dimensional convection-diffusion problem. M2AN Math. Model. Numer. Anal., 33, (1999) pp. 493-516.

[3] R.Eymard, T.Gallouet, R.Herbin, Finite Volume Methods, in: Handbook for Numerical Analysis, Vol. 7 (Ph.Ciarlet, J.L.Lions, eds.), Elsevier, 2000.

[4] O.Drblíková, K.Mikula, Convergence analysis of finite volume scheme for nonlinear tensor anisotropic diffusion in image processing, SIAM Journal on Numerical Analysis, Vol. 46, No.1 (2007) pp. 37-60.

[5] O.Drblíková, A.Handlovičová, K.Mikula, Error estimates of the finite volume scheme for the nonlinear tensor-driven anisotropic diffusion, Applied Numerical Mathematics, Vol. 59, No. 10 (2009) pp. 2548-2570

[6] D.Kuzmin, Linearity-preserving flux correction and convergence acceleration for constrained Galerkin schemes, Journal of Computational and Applied Mathematics, 2011, http://dx.doi.org/10.1016/j.cam.2011.11.019

[7] K.Mikula, M.Ohlberger, A new level set method for motion in normal direction based on a semi-implicit forward-backward diffusion approach, SIAM J. Scientific Computing, Vol. 32, No. 3 (2010) pp. 1527-1544

[8] K.Mikula, M.Ohlberger, A new Inflow-Implicit/Outflow-Explicit Finite Volume Method for Solving Variable Velocity Advection Equations, Preprint 01/10 - N, Angewandte Mathematik und Informatik, Universitaet Münster, June 2010.

[9] K.Mikula, M.Ohlberger, Inflow-Implicit/Outflow-Explicit Scheme for Solving Advection Equations, in Finite Volumes in Complex Applications VI, Problems & Perspectives, Eds. J.Fořt et al. (Proceedings of the Sixth International Conference on Finite Volumes in Complex Applications, Prague, June 6-10, 2011), Springer Verlag, 2011, pp. 683-692.

[10] K.Mikula, M.Ohlberger, J.Urbán, Inflow-Implicit/Outflow-Explicit Finite Volume Methods for Solving Advection Equations, Technical Report 01/12 - N , FB 10 , Universitaet Muenster, Number 01/12 - N - February 2012

[11] S.T.Zalesak: Fully multidimensional flux-corrected transport algorithms for fluids, J. Comput. Phys., Vol. 31 (1979) pp.335-362